Ultra-strong through-space conjugation enabled by robust molecular skeleton and flexible aggregate

Qingyang Xu[1,2,3,#], Jianyu Zhang[4,#], Jing Zhi Sun[1,3], Haoke Zhang[1,2,3,*], Ben Zhong Tang[1,4,5*]

[1]MOE Key Laboratory of Macromolecular Synthesis and Functionalization, Department of Polymer Science and Engineering, Zhejiang University, Hangzhou 310058, China

[2]Zhejiang-Israel Joint Laboratory of Self-Assembling Functional Materials, ZJU-Hangzhou Global Scientific and Technological Innovation Center, Zhejiang University, Hangzhou 311215, China

[3]Centre of Healthcare Materials, Shaoxing Institute, Zhejiang University, Shaoxing 312000, China

[4]Department of Chemistry, Hong Kong Branch of Chinese National Engineering Research Center for Tissue Restoration and Reconstruction, The Hong Kong University of Science and Technology, Hong Kong, 999077, China

[5]School of Science and Engineering, Shenzhen Institute of Aggregate Science and Technology, The Chinese University of Hong Kong, Shenzhen (CUHK-Shenzhen), Guangzhou 518172, China

[#]These authors contributed equally

Corresponding emails: zhanghaoke@zju.edu.cn (Haoke Zhang) tangbenz@cuhk.edu.cn (Ben Zhong Tang)

Abstract: Manipulating the electronic structure of organic functional materials by through-space conjugation (TSC) to achieve high photophysical performances has been a longstanding research focus. Although the working mechanisms of TSC have been demonstrated, the fundamental roles of the intrinsic molecular skeleton and extrinsic aggregates remain unclear. Herein, four trinaphthylmethanol (TNMOH) isomers and four trinaphthylmethane (TNM) isomers with varying connecting sites of naphthalene were synthesized, and their photophysical properties were systematically investigated. The strength of TSC gradually enhanced from 222-TNM to 111-TNM with the increased number of 1-naphthalene units, resulting in long-wavelength clusteroluminescence with an absolute quantum yield of 57% of 111-TNM. Experimental and theoretical results revealed that the inherent attribute of robust intramolecular interactions within individual molecules is fundamental for ultra-strong TSC, and intermolecular interactions play an auxiliary role in fortifying and stabilizing intramolecular interactions. This work demonstrates the intrinsic and extrinsic factors of manipulating TSC and provides a reliable strategy for constructing nonconjugated luminogens with efficient clusteroluminescence.

Introduction

The electronic structure of matter has a profound impact on its properties.[1-3] For example, electronic-structure modifications can significantly influence various characteristics, such as catalytic activity,[4] conductivity,[5] optical properties,[6,7] and reaction reactivity.[8] Therefore, manipulating the electronic structure of materials to achieve high performance has been a longstanding research focus. Generally, the prerequisite for controlling the electronic structure lies in the ability of electrons to undergo delocalization within the molecular framework.[9,10] This delocalization can be achieved through two main approaches: through-bond conjugation (TBC) and through-space conjugation (TSC).[11-13] During the past several decades, TBC-based theories have been applied successfully to regulate the electronic structure of traditionally conjugated molecules, leading to the superior performance of many organic functional materials.[14-16] However, the specific processes and mechanisms by which TSC influences the electronic structure and subsequently affects material properties remain elusive.

Usually, extended conjugation of organic molecules is the cornerstone to achieve efficient luminescence with visible or near-infrared emission. Nevertheless, some natural nonconjugated materials without aromatic rings or large π-conjugated structures, such as starch, cellulose, and peptides, can also emit visible light.[17-20] These materials do not exhibit luminescence in the isolated state but display intriguingly visible light known as clusteroluminescence (CL) in the aggregate state.[19,21,22] Previous reports have suggested the significant role of TSC in promoting CL,[23-26] but there is still a lack of in-depth and systematic research on the relationship among electronic structure, aggregate structure, and properties based on TSC, presenting challenges in the precise control of emission color and efficiency of materials with CL property. Fortunately, multiaryl-substituted alkanes (MAAs) with well-defined structural conformation and high purity compared to polymers offer an excellent platform for studying TSC.[27] Previous studies have already reported the structure-property relationship of TSC in some MAAs, such as diphenylmethane,[28] triphenylmethane,[25] and tetraphenylethane.[24] However, the efficiency of TSC in these systems is still low and shows unstable characteristics, exhibiting difficulties in promoting ultra-strong TSC. Specifically, it has been reported that the flexibility of aggregate exerted a significant influence on TSC, but the mechanisms and contributions from intrinsic and extrinsic factors were ambiguous.[29-31] Therefore, in-depth research on regulating the rigidity and flexibility of aggregate to achieve ultra-strong TSC and investigating the underlying reasons behind them are essential.

In this work, four trinaphthylmethanol (TNMOH) isomers and four trinaphthylmethane (TNM) isomers have been successfully synthesized and satisfactorily characterized (Fig. 1 and Supplementary Figs. S1-20), and their photophysical properties were systematically studied. They all show typical intrinsic short-wavelength emission from naphthalene in dilute solution and another long-wavelength emission from TSC in the aggregate state. Compared to TNMOH isomers, TNM isomers exhibit stronger TSC which is further strengthened from 222-TNM to

111-TNM with the increased number of 1-naphthalene units. Remarkably, solid-state 111-TNM displays ultra-stable and highly efficient TSC, resulting in the TSC-dominant emission with an absolute luminescence quantum yield (Φ_{solid}) of 57%. Experimental results and theoretical calculations demonstrate that 111-TNM displays maximum rigidity of intrinsic molecular skeleton but the highest degree of flexibility of aggregate due to weak intermolecular interactions. This result suggests that strong intramolecular interactions predominantly account for the ultra-strong TSC behavior. In addition, the flexibility of aggregate is governed by intermolecular interactions, rather than the intrinsic characteristics of individual molecule. This work not only leads to a deeper understanding of the properties of aggregate but also provides a reliable strategy for constructing ultra-strong TSC materials.

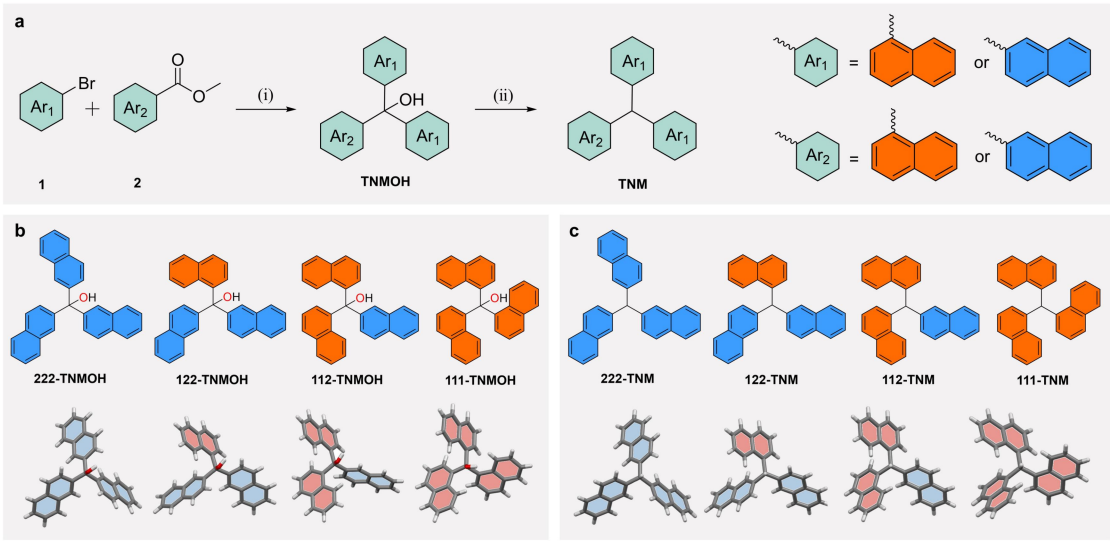

Fig. 1 Synthesis and single-crystal structures of TNMOH and TNM isomers. a) Synthesis procedures, reagents, and conditions: (i) *n*-BuLi, THF, -78°C to room temperature (rt); (ii) $InCl_3$, $HSiClMe_2$, CH_2Cl_2, rt, 15 min. Chemical structures and single-crystal structures of b) TNMOH isomers and c) TNM isomers.

Results

Photophysical properties of TNMOH. The photophysical properties of four TNMOH isomers with three isolated naphthyl rings were first studied. All four isomers exhibit typical absorption peaks from naphthyl rings located at about 280 nm in pure acetonitrile (ACN) solution (Supplementary Fig. S21). Adding water to the solution causes the formation of aggregates, resulting in a slight redshift of absorption. Subsequently, the photoluminescence (PL) performance of TNMOH isomers in ACN/water mixtures was investigated. 222-TNMOH only exhibits an emission peak at 339 nm in pure ACN solution, corresponding to the intrinsic emission from the naphthalene ring (Fig. 2a).[32] Its intensity gradually increases with the increased water fraction (f_w), which reaches its maximum at f_w = 70% due to the enhanced polarity of the solution.[24,33] Further increasing f_w leads to the formation of aggregates, resulting in a decrease of the original peak at 339 nm and the appearance of a broad peak at 400 nm. According to previous work, this emerging new long-wavelength emission can be attributed to the formation of intramolecular weak TSC

among isolated naphthalene rings.[24,25] The other three TNMOH isomers display similar properties to 222-TNMOH (Fig. 2b-d). Interestingly, a linear relationship between relative PL intensity (I/I_0) and f_w is observed before the formation of aggregates (Fig. 2e), which indicates that the increase in solvent polarity is directly proportional to the enhancement of fluorescence intensity.[34] Furthermore, in this stage (before the formation of aggregates), the rate of PL intensity enhancement follows the order of 222-TNMOH > 122-TNMOH > 112-TNMOH > 111-TNMOH. It is speculated that the flexible conformation of 222-TNMOH has the strongest interaction with the solvent molecules, while the most crowded structure of 111-TNMOH shows the weakest interaction with its surrounding solvent molecules, resulting in their different responsiveness to solvent polarity. In the solid state, all TNMOH isomers exhibit a distinct emission peak with a board shoulder around 331-520 nm (Fig. 2f), which corresponds to the emission from the naphthalene ring and a subtle presence of TSC formed among isolated naphthalene rings. However, it is noteworthy that the formed TSC is comparatively weak in both aggregate and solid states, so no pronounced emission peak from TSC is observed.

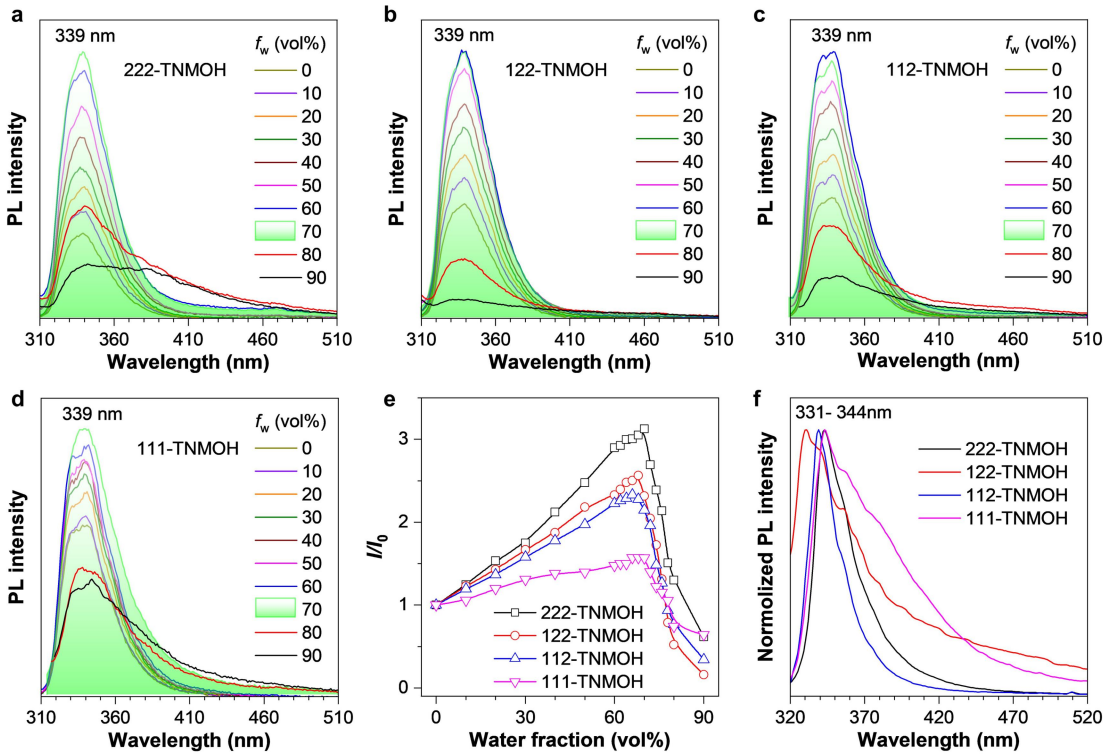

Fig. 2 Photophysical properties of TNMOH isomers. Photoluminescence (PL) spectra of a) 222-TNMOH, b) 122-TNMOH, c) 112-TNMOH, and d) 111-TNMOH in ACN/water mixtures with different water fractions (f_w). Concentration = 10 μM. e) Plots of relative PL intensity (I/I_0) versus different f_w at the emission wavelength of 339 nm. I_0 = PL intensity at f_w = 0%. f) PL spectra of TNMOH isomers in the solid state.

Photophysical properties of TNM. Similar to TNMOH isomers, all four TNM isomers display the typical absorption peaks from three isolated naphthyl rings at around 280 nm (Fig. 3a-d and Supplementary Fig. 21). In pure ACN solution, they all exhibit an emission peak solely at 339 nm

(Fig. 3e-h). With the increased f_w in ACN/water mixtures, the PL intensity of the intrinsic peak gradually enhances, reaching its maximum at f_w = 60%. However, after the formation of aggregates at $f_w \geq 70\%$, their PL properties are different from TNMOH isomers and could be divided into two types: (i) For 222-TNM and 122-TNM, a weak shoulder peak extending to 500 nm is observed, indicating the presence of weak and unstable TSC according to previous report (Fig. 3e-f).[25] (ii) Conversely, 112-TNM and 111-TNM show a strong and broad emission peak within the visible-light range (Fig. 3g-h). At f_w = 90%, the peak intensity of 112-TNM at 384 nm is 25 times higher than that in pure ACN solution (Fig. 3k), and the peak intensity of 111-TNM at 395 nm reaches 41 times higher (Fig. 3l). These results indicate that aggregates of 112-TNM and 111-TNM are able to produce ultra-strong TSC. Meanwhile, it is noteworthy that the aggregation-induced TSC emission in 112-TNM and 111-TNM is different from the reported excimer emission (broad peak) in π-conjugated planar chromophores. These TSC emission peaks exhibit fine structures, suggesting stronger interaction of intramolecular TSC than the general intermolecular π-π interaction.

The different strengths of TSC of these four TNM isomers inspired us to explore the PL properties of their solid-state samples. Interestingly, only the intrinsic emission peak at 339 nm from the naphthalene moiety is observed in 222-TNM, and no long-wavelength peak is detected (Fig. 3m). For 122-TNM, a long-wavelength peak appears at 375 nm, but its intensity is weaker than the intrinsic peak at 343 nm (Fig. 3n). However, the long-wavelength emission becomes dominant in 112-TNM and 111-TNM, which located at 380 nm and 393 nm with deep purple color, respectively (Fig. 3o-p and Supplementary Figs. S24-25). Notably, the emission peak of TSC is significantly stronger than that of the intrinsic peak at 340 nm from the naphthalene moiety. These findings indicate that the strength of TSC is gradually enhanced with the increasing number of 1-naphthalene units, and 111-TNM reaches the maximum, demonstrating the crucial role of 1-naphthalene in generating intramolecular TSC.

To verify the fundamental feature and modulation of TSC, different experimental conditions were further implemented. First, increasing the concentration of mixtures can significantly promote the formation of aggregates for all TNM isomers. As expected, the long-wavelength emission from TSC is also enhanced (Supplementary Figs. S26-29). Significantly, the intensity ratio of the maximum TSC peak to the maximum intrinsic emission from naphthalene is gradually increased with the increase of concentration. For example, in 111-TNM, these two peaks almost have the same intensity at c = 100 μM (Supplementary Figs. S29). On the other hand, reducing the polarity of the favorable solvent notably diminishes the stability of TSC (Supplementary Figs. S30-33). For instance, 111-TNM only displays the long-wavelength emission in THF/water mixtures with f_w = 90%. These results suggest that high concentration and increased polarity of the favorable solvent facilitate the formation of aggregates, leading to restricted intramolecular motions and the establishment of stable TSC. As a comparison, increasing the concentration of 111-TNMOH fails to induce strong TSC (Supplementary Fig. S34). Thereby, it is believed that the

presence of robust TSC in the aggregate state is the inherent property of molecule, while external conditions also play an essential role in adjusting its strength.

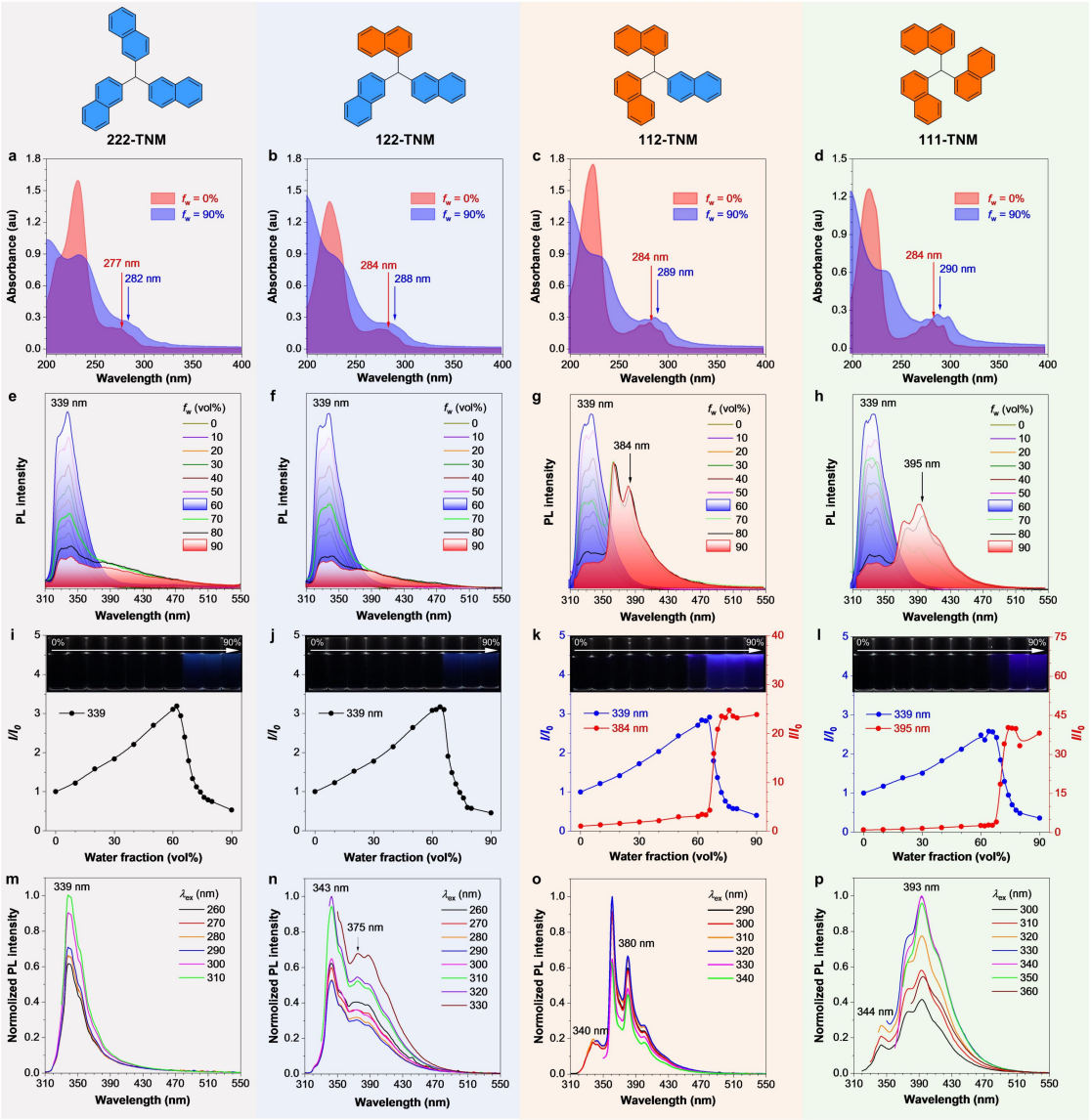

Fig. 3 Photophysical properties of TNM isomers. Absorption spectra of a) 222-TNM, b) 122-TNM, c) 112-TNM, and d) 111-TNM in ACN/water mixtures with different water fractions (f_w). Concentration (c) = 10 μM. Photoluminescence (PL) spectra of e) 222-TNM, f) 122-TNM, g) 112-TNM, and h) 111-TNM in ACN/water mixtures with different f_w, c = 10 μM. i-l) Plots of relative PL intensity (I/I_0) of different maximum emission wavelengths versus different f_w. Inset: fluorescent photo of TNM isomers in ACN/water mixtures taken under the illumination of a 254 nm UV lamp. PL spectra of solid-state m) 222-TNM, n) 122-TNM, o) 112-TNM, and p) 111-TNM under different excitation wavelengths.

Comparison of photophysical properties between TNMOH and TNM isomers. The photophysical properties of TNMOH and TNM isomers were systematically summarized in Table 1. The absorption wavelengths of each pair of TNMOH and TNM are almost the same. For example, 222-TNMOH with λ_{abs} of 277/283 nm exhibited a high degree of consistency with those of 222-TNM with λ_{abs} of 277/282 nm. The result indicates that the introduction of a hydroxyl group to TNM minimally affects their ground-state properties. However, their excited-state properties of luminescence are different. Although they all show the intrinsic emission from the naphthalene unit at 339 nm in pure ACN solution, the long-wavelength emission from ultra-strong TSC is observed at 384 nm and 395 nm in the aggregate state of 112-TNM and 111-TNM, respectively. In contrast, such emission is absent in 112-TNMOH and 111-TNMOH. Especially, the emission from TSC is more obvious in the solid-state TNM isomers (except 222-TNM) but totally disappears in the TNMOH counterparts. This observation clearly suggests that the presence of a hydroxyl group would destroy TSC, thereby influencing the PL properties of these molecules.

Table 1. Photophysical properties of TNMOH and TNM isomers

Compounds	$\lambda_{abs,\ solution}$ (nm)		$\lambda_{ex,\ solution}$ (nm)		$\lambda_{em,\ solution}$ (nm)		α_{AIE}	$\lambda_{em,\ solid}$ (nm)	Φ_{solid} (%)	τ_{solid} (ns)	
	f_w = 0%	f_w = 90%	f_w = 0%	f_w = 90%	f_w = 0%	f_w = 90%				339 nm	390 nm
222-TNMOH	277	283	285	293	339	~340	/	343	20	21.0	22.2
122-TNMOH	281	286	288	296	339	~340	/	332	< 1%	7.1	9.6
112-TNMOH	282	287	292	299	339	~340	/	339	10	16.8	16.9
111-TNMOH	284	289	295	303	339	~340	/	344	8	3.4	5.3
222-TNM	277	282	285	293	339	~340	/	340	10	40.7	43.9
122-TNM	284	288	288	295	339	~340	/	343/375	61	9.1	11.1
112-TNM	284	289	295	300/300	339	~340/384	25	340/380	68	5.5	8.3
111-TNM	284	290	296	302/302	339	~340/395	41	344/393	57	4.1	9.7

$\lambda_{abs,\ solution}$: maximum absorption wavelength in ACN/water mixtures, λ_{ex}: excitation wavelength in ACN/water mixtures (Supplementary Fig. S22-23), $\lambda_{em,\ solution}$: maximum emission wavelength in ACN/water mixtures, $\lambda_{em,\ solid}$: maximum emission wavelength in the solid state, f_w: water fraction of ACN/water mixtures, α_{AIE}: relative PL intensity (I_{90}/I_0) at λ_{em} = 384 nm or 395 nm, I_0: PL intensity at f_w = 0%, I_{90}: PL intensity at f_w = 90%, Φ_{solid}: absolute luminescence quantum yield in the solid state, τ_{solid}: emission lifetime in the solid state.

The solid-state absolute luminescence quantum yields (Φ_{solid}) of 122-TNM (61%), 112-TNM (68%), and 111-TNM (57%) are significantly higher than 222-TNM (10%), which can be attributed to the enhanced stability of TSC resulting from the increased number of 1-naphthalene units. In contrast, the Φ_{solid} of 222-TNMOH (20%), 122-TNMOH (<1%), 112-TNMOH (10%), and 111-TNMOH (8%) are markedly low. This disparity may be attributed to the involvement of *n* electrons in the oxygen atom of the hydroxyl group, leading to the theoretically forbidden (n, π^*) transition with small oscillator strength. The time-solved decay of both TNMOH and TNM isomers revealed that all emission exhibit fluorescent characteristics (Supplementary Figs.

S35-36). Notably, the lifetimes of the long-wavelength emission from TSC consistently surpass the short-wavelength emission, indicating another relaxing process of excitons to the stable state of TSC.

Single-molecule and crystalline analysis of TNM isomers. To illustrate the underlying difference among TNM isomers and the remarkably strong TSC of 112-TNM and 111-TNM, theoretical calculations based on single-molecule and crystalline models were performed using the time-dependent density functional theory (TD-DFT) method. Root-mean-square deviation (RMSD), referring to the atomic positional changes between the optimized ground and excited states, was first utilized to evaluate the intrinsic rigidity of these compounds. As expected, 222-TNM exhibits flexible conformation and pronounced molecular motion with a large RMSD value of 1.3362 Å (Fig. 4a) in the single-molecule state. Compared to 222-TNM, due to the introduction of 1-naphthalene units, both 122-TNM (0.4823 Å) and 112-TNM (0.5469 Å) display restricted intramolecular motion with reduced RMSD values. Moreover, 111-TNM exhibits an extremely small RMSD value of 0.1909 Å, indicating the highest rigidity of molecular skeleton among the four TNM isomers. In addition, reorganization energy (λ), serving as a quantitative indicator of the inherent geometric alteration upon photoexcitation, can also reflect contributions of intramolecular motions to nonradiative decay.[35,36] As expected, the total λ of 222-TNM is determined to be 6879 cm^{-1} with 63.36% from twisting motions of dihedral angle (Fig. 4b). In contrast, 111-TNM exhibits the smallest λ (2176 cm^{-1}) and the smallest proportion from motions of dihedral angle (10.58%), supporting its rigid skeleton. Therefore, both RMSD and reorganization analysis demonstrate the order of intrinsic rigidity of these four TNM isomers as 222-TNM < 112-TNM < 122-TNM < 111-TNM.

Since TSC was closely related to the aggregate state, the crystalline phase of TNM isomers was subsequently examined. In the crystal structure of 222-TNM, an intriguing phenomenon is observed that two 222-TNM molecules bound together, forming an interlocked structure with three arms (Fig. 4c). Each naphthalene ring is almost perpendicular to an adjacent naphthalene of the other molecule. The distances of d_1 (2.645 Å) and d_2 (2.776 Å) indicate the presence of strong $C-H\cdots\pi$ interactions. These interactions are also clearly visualized from the Hirshfeld surface, where six red spots highlighted interactions between the two 222-TNM molecules (Fig. 4d).[37,38] However, the distances between the other three molecules (d_3-d_{11}) and their corresponding Hirshfeld surfaces indicate that their crystal packings are not as tight as 222-TNM. In particular, only one strong interaction of 111-TNM with its surrounding another molecule is observed (Supplementary Figs. S37-40). In addition, analysis of reorganization energy in the crystalline phase supports the above results. For example, the total λ of 222-TNM decreases from 6879 cm^{-1} in the gas phase to 1821 cm^{-1} in the crystalline phase, while 111-TNM shows the smallest decrease from 2176 cm^{-1} to 2076 cm^{-1}. This substantial decrease indicates that the intermolecular interactions strongly restrict the molecular motions of 222-TNM in the aggregate state, whereas the motions of 111-TNM are less constrained. Besides, 122-TNM (from 2341 cm^{-1} to 1958 cm^{-1})

and 112-TNM (from 3114 cm^{-1} to 2024 cm^{-1}) exhibit a moderate λ decrease from gas phase to crystalline phase. Therefore, the order of flexibility induced by intermolecular interactions in the aggregate state can be summarized as follows: 222-TNM < 122-TNM < 112-TNM < 111-TNM. Combining single-molecule and crystalline analysis of TNM isomers, 222-TNM exhibits the highest flexibility of the single-molecule skeleton but the highest rigidity of aggregate. On the contrary, 111-TNM shows the most rigid skeleton but the most flexible of aggregate due to weak intermolecular interactions. The above results suggest the independence of intrinsic rigidity of molecular skeleton and flexibility of aggregate.

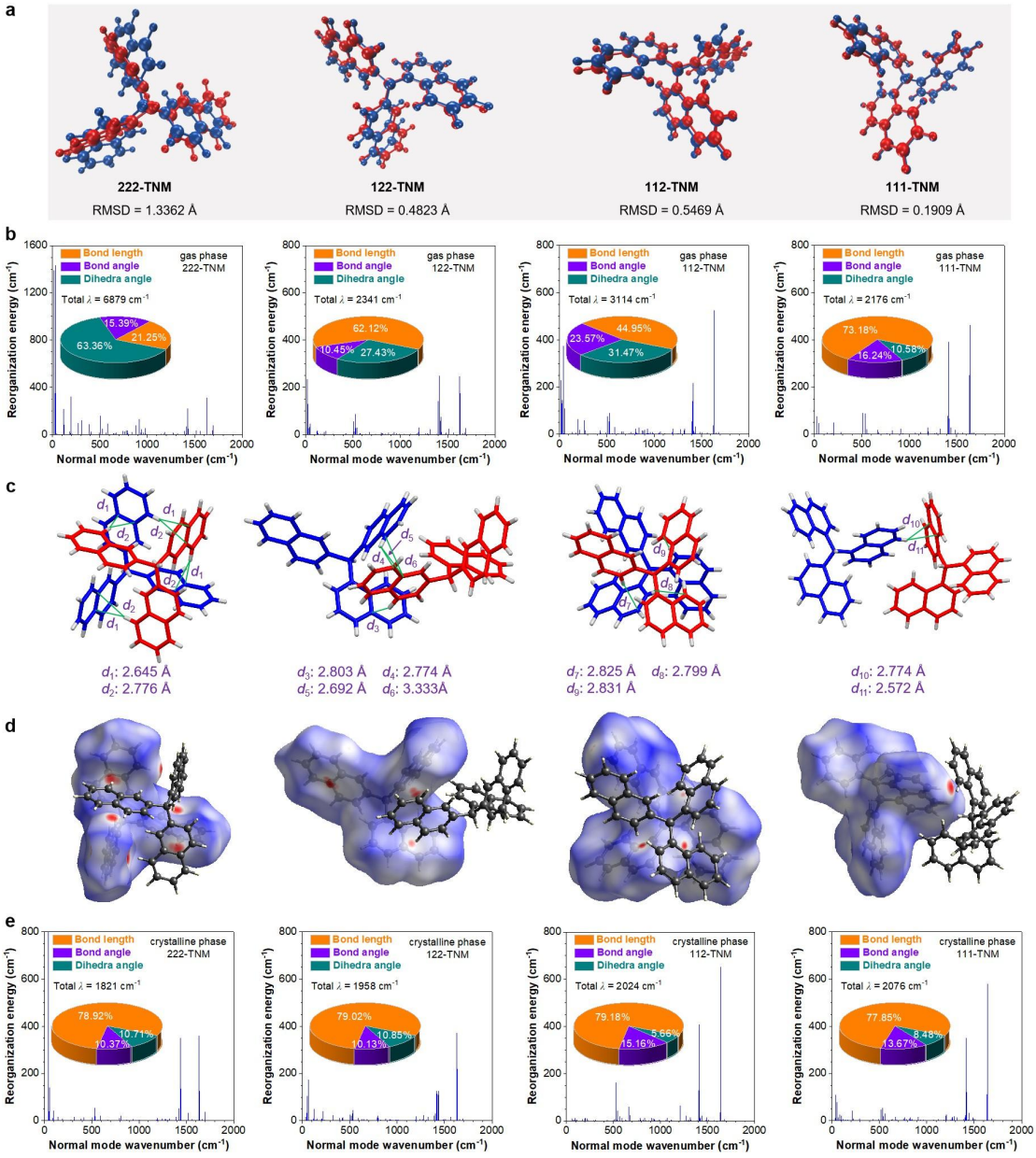

Fig. 4 Gas and crystalline phase analysis of TNM isomers. a) Overlaps of the optimized ground-state (blue color) and excited-state (red color) geometries of TNM isomers in the gas phase. The root-mean-square deviation (RMSD) of atomic positions was calculated to evaluate the strength of intramolecular motions in two different states. b) Plots of reorganization energy versus

normal mode wavenumber of TNM isomers in the gas phase. Inset: Proportions of bond length, bond angle, and dihedral angle contributed to total reorganization energy. c) Typical dimers of TNM isomers from their corresponding crystal-packing structures. d) Hirshfeld surfaces (mapped over d_{norm}) of TNM isomers. e) Plots of reorganization energy versus normal mode wavenumber of TNM isomers in the crystalline phase. Inset: Proportions of bond length, bond angle, and dihedral angle contributed to total reorganization energy.

Intramolecular interactions analysis of TNM isomers. Theoretically, the ultra-strong TSC can stem from intermolecular interactions, intramolecular interactions, or a combination of both. As discussed above, weak intermolecular interactions of 111-TNM indicate that its ultra-strong TSC should be attributed to intramolecular interactions rather than intermolecular ones. To prove this speculation, the temperature-dependent PL spectra of 111-TNM in dilute solutions were investigated, which could rule out the influence of intermolecular interactions.[41] As shown in Fig. S45a, 111-TNM only shows an intrinsic naphthalene emission at room temperature, however, a long-wavelength emission peak resulting from TSC emerged upon reducing the temperature (Supplementary Fig. S45). The theoretical calculation on the intermolecular interactions and temperature-dependent PL spectra indicate that the TSC of TNM is an intrinsic characteristic originating from intramolecular interactions among isolated naphthalene rings.

Therefore, intramolecular interactions of TNM isomers were further explored. Through-space intramolecular interactions could be identified if the distances between atoms separated by more than three bonds are shorter than the sum of van der Waals radii.[39,40] Accordingly, two types of intramolecular interactions are distinguished from this system, including hydron-involved interactions (HII) and carbon-carbon interactions (CCI). Generally, the larger number of HII and CCI correspond to the stronger intramolecular rigidification and TSC, respectively. The results show that these intramolecular interactions are gradually strengthened from 222-TNM to 111-TNM with the increased number of 1-naphthalene units. For example, 222-TNM, 122-TNM, 112-TNM and 111-TNM show 3, 8, 12 and 16 pairs of HII. The larger paris of CCI in 112-TNM and 111-TNM than that of 222-TNM and 122-TNM also proves the stronger TSC in 112-TNM and 111-TNM (Fig. 5a).

The role of intermolecular interactions at aggregate state for strong TSC was further considered. According to the core mechanism of aggregation-induced emission phenomenon, vigorous molecular motions within dilute solutions result in the instability of intramolecular interactions, which destroy TSC and quench emission. The establishment of stable intramolecular interactions and TSC requires external forces. Therefore, both the formation of aggregates and the decrease in temperature can restrict the motions of individual molecule, leading to stable intramolecular interactions and strong TSC. Based on this conclusion, it can be inferred that stable intramolecular interactions in room-temperature dilute solutions may be achieved by introducing stronger steric hindrance to individual molecule, which is the focus of our future endeavors.

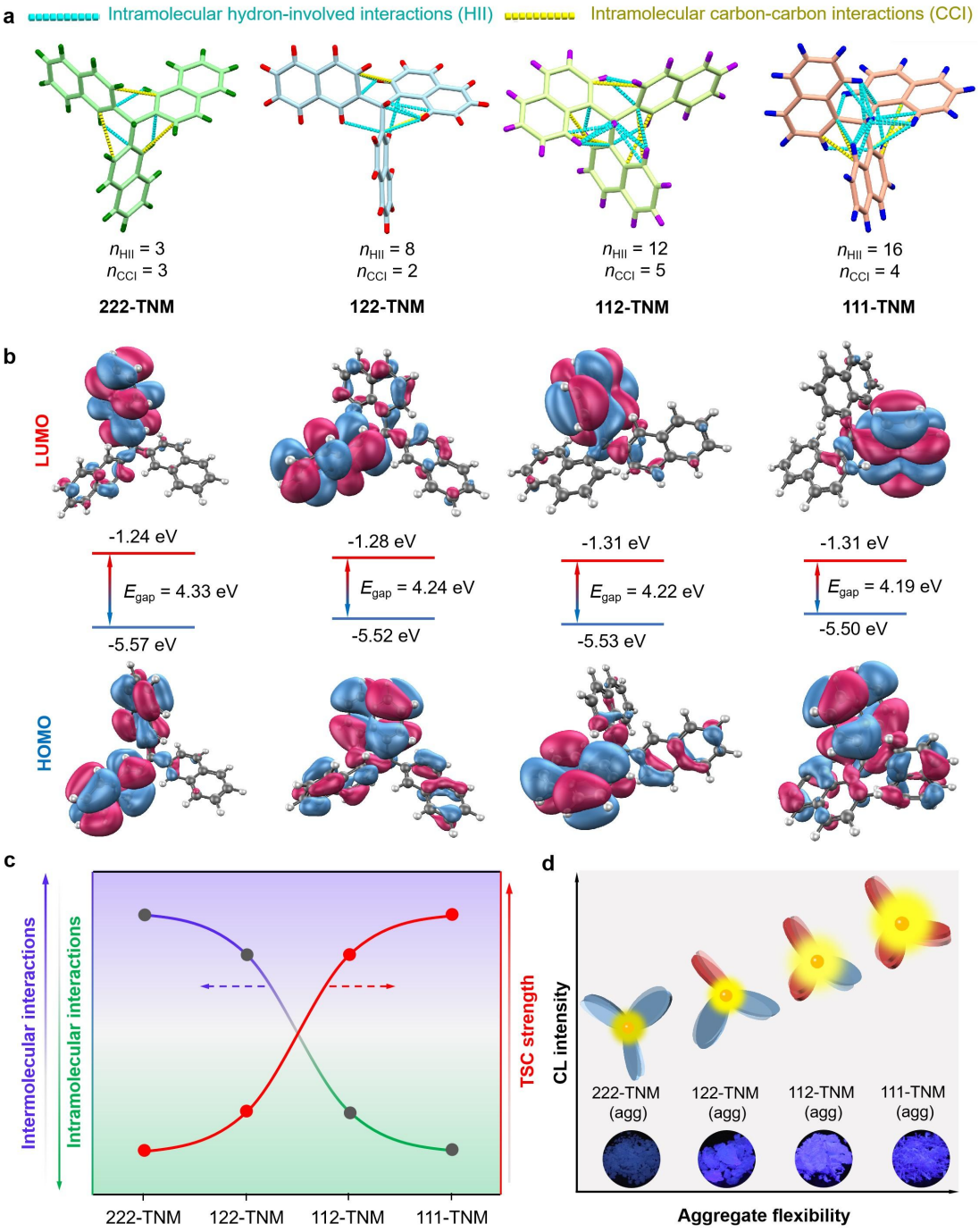

Fig. 5 Intramolecular interactions of TNM isomers. a) Intramolecular interactions of TNM isomers in the crystalline phase. n_{HII}: number of intramolecular hydron-involved interactions. n_{CCI}: number of intramolecular carbon-carbon interactions. b) Frontier molecular orbitals of TNM isomers based on the optimized excited-state geometries in crystalline phase calculated by TD-DFT method at the B3LYP-D3/6-31G(d,p) level, Gaussian 09 program. c) Schematic plot of the relationship between intramolecular and intermolecular interactions and the strength of TSC. d) Schematic plot of the relationship between the aggregate flexibility and CL intensity of TNM isomers. Inset: fluorescent photos of TNM isomers in the solid state captured under a 254 nm UV lamp.

Moreover, the frontier molecular orbitals and energy gap based on the optimized excited-state geometries of TNM isomers in the crystalline phase were calculated (Fig. 5b, Supplementary Fig. S46-48). It is obvious that electrons can delocalize between three isolated naphthalene rings, suggesting the feature of TSC. Besides, the calculated energy gaps gradually decrease from 4.33 eV of 222-TNM to 4.19 eV of 111-TNM, closely correlated with the enhancement of TSC and redshift of corresponding emission. According to the above results, a schematic diagram for TSC of TNM isomer could be summarized (Fig. 5c). From 222-TNM, 122TNM to 112-TNM and 111-TNM with the increased number of 1-naphthalene units, there is a notable decrease in strength of intermolecular interactions accompanied by a significant increase in strength of intramolecular interactions. This progressive shift results in the gradual stabilized and amplified TSC, as evidenced by the increased efficiency and intensity of visible emission from TSC (Fig. 5d). These findings clearly confirm that the ultra-strong TSC originates primarily from the strengthening of intramolecular interactions, while intermolecular interactions play a vital role in stabilizing intramolecular interactions.

Conclusions

In this work, four TNMOH isomers and four TNM isomers with nonconjugated naphthalene rings were synthesized to thoroughly investigate the modulation of TSC. They all show intrinsic emission from naphthalene in dilute solution, but their photophysical properties in the aggregate state are different. Although TNMOH isomers exhibit weak TSC due to introducing a hydroxyl group, TNM isomers show ultra-strong TSC with efficiency CL. Significantly, the strength of TSC gradually enhanced from 222-TNM to 111-TNM with the increased number of 1-naphthalene units, promoting the TSC-dominant emission of 111-TNM with an impressive quantum efficiency of 57% in the solid state. Experimental investigations and theoretical calculations elucidate that the inherent attribute of robust intramolecular interactions within individual molecule is fundamental for ultra-stable TSC, and intermolecular interactions play an auxiliary role in fortifying and stabilizing intramolecular interactions. This work not only unveils the intrinsic and extrinsic parts of manipulating TSC, but also provides a novel strategy for achieving ultra-stable TSC and highly efficient CL. The mechanistic investigation may further help understand the processes and mechanisms of modulating electronic structure and photophysical properties.

Data availability

The crystallographic data for the structures reported in this article have been deposited at the Cambridge Crystallographic Data Centre (CCDC) under deposition numbers 2272325 (222-TNMOH), 2272326 (122-TNMOH), 2272327 (112-TNMOH), 2272328 (111-TNMOH), 2272329 (222-TNM), 2272330 (122-TNM), 2272331 (112-TNM), and 2272332 (111-TNM). These data can be obtained free of charge from CCDC via www.ccdc.cam.ac.uk/data_request/cif.

All other data supporting the findings of this study are available within the manuscript and Supplementary Information.

Acknowledgments

This work is supported by the National Science Foundation of China (grant no. 22205197), and the Youth Talent Excellence Program of ZJU-Hangzhou Global Scientific and Technological Innovation Center. J. Zhang acknowledged the support from the Research Grants Council Postdoctoral Fellowship Scheme of the Hong Kong Special Administrative Region, China (HKUST PDFS2324-6S01).

Author contributions

Q.Y.X. and H.K.Z. conceived and designed the experiments. Q.Y.X. performed the synthesis and the photophysical measurements. J.Y.Z. conducted theoretical calculations. Q.Y.X., J.Y.Z. and H.K.Z. analyzed the data. Q.Y.X, J.Y.Z., H.K.Z, J.Z.S. and B.Z.T. took part in the discussion and gave important suggestions. Q.Y.X., J.Y.Z. and H.K.Z. co-wrote the paper.

Competing interests

The authors declare no competing interests.

Reference

1. Fokin, A. A.; Gerbig, D.; Schreiner, P. R., sigma/sigma- And pi/pi-interactions are equally important: multilayered graphanes. *J. Am. Chem. Soc.* **2011**, *133* (50), 20036-9.

2. Ai, X.; Evans, E. W.; Dong, S.; Gillett, A. J.; Guo, H.; Chen, Y.; Hele, T. J. H.; Friend, R. H.; Li, F., Efficient radical-based light-emitting diodes with doublet emission. *Nature* **2018**, *563* (7732), 536-540.

3. Ma, S.; Du, S.; Pan, G.; Dai, S.; Xu, B.; Tian, W., Organic molecular aggregates: From aggregation structure to emission property. *Aggregate* **2021**, *2*, e96.

4. Deng, D.; Novoselov, K. S.; Fu, Q.; Zheng, N.; Tian, Z.; Bao, X., Catalysis with two-dimensional materials and their heterostructures. *Nat. Nanotechnol.* **2016**, *11* (3), 218-30.

5. Sun, L.; Campbell, M. G.; Dinca, M., Electrically Conductive Porous Metal-Organic Frameworks. *Angew. Chem. Int. Ed.* **2016**, *55* (11), 3566-79.

6. Sun, S.; Lu, M.; Gao, X.; Shi, Z.; Bai, X.; Yu, W. W.; Zhang, Y., 0D Perovskites: Unique Properties, Synthesis, and Their Applications. *Ad.v Sci.* **2021**, *8* (24), e2102689.

7. Cai, X.-M.; Zhong, W.; Deng, Z.; Lin, Y.; Tang, Z.; Zhang, X.; Zhang, J.; Wang, W.; Huang, S.; Zhao, Z.; Tang, B. Z., A simple AIE-active salicylideneaniline towards bimodal encryption-decryption with unique ESIPT-inhibited amorphous state. *Chem. Eng. J.* **2023**, *466*, 143353.

8. Li, X. H.; Antonietti, M., Metal nanoparticles at mesoporous N-doped carbons and carbon nitrides: functional Mott-Schottky heterojunctions for catalysis. *Chem. Soc. Rev.* **2013**, *42* (16), 6593-604.

9. Yamaguchi, Y.; Matsubara, Y.; Ochi, T.; Wakamiya, T.; Yoshida, Z., How the pi conjugation length affects the fluorescence emission efficiency. *J. Am. Chem. Soc.* **2008**, *130* (42), 13867-13869.

10. Guo, J.; Xu, Y.; Jin, S.; Chen, L.; Kaji, T.; Honsho, Y.; Addicoat, M. A.; Kim, J.; Saeki, A.; Ihee, H.; Seki, S.; Irle, S.; Hiramoto, M.; Gao, J.; Jiang, D., Conjugated organic framework with three-dimensionally ordered stable structure and delocalized pi clouds. *Nat. Commun.* **2013**, *4*, 2736.

11. Saal, F.; Zhang, F.; Holzapfel, M.; Stolte, M.; Michail, E.; Moos, M.; Schmiedel, A.; Krause, A. M.; Lambert, C.; Wurthner, F.; Ravat, P., [n]Helicene Diimides (n = 5, 6, and 7): Through-Bond versus Through-Space Conjugation. *J. Am. Chem. Soc.* **2020**, *142* (51), 21298-21303.

12. Li, J.; Zhuang, Z.; Shen, P.; Song, S.; Tang, B. Z.; Zhao, Z., Achieving Multiple Quantum-Interfered States via Through-Space and Through-Bond Synergistic Effect in Foldamer-Based Single-Molecule Junctions. *J. Am. Chem. Soc.* **2022**, *144* (18), 8073-8083.

13. Hoffmann, R., Interaction of orbitals through space and through bonds. *Acc. Chem. Res.* **1971**, *4* (1), 1-9.

14. Xie, L. S.; Skorupskii, G.; Dinca, M., Electrically Conductive Metal-Organic Frameworks. *Chem. Rev.* **2020**, *120* (16), 8536-8580.

15. Fang, F.; Jiang, Q.; Klausen, R. S., Poly(cyclosilane) Connectivity Tunes Optical Absorbance. *J. Am. Chem. Soc.* **2022**, *144* (17), 7834-7843.

16. Cai, X.-M.; Lin, Y.; Tang, Z.; Zhang, X.; Mu, T.; Huang, S.; Zhao, Z.; Tang, B. Z., Filling the gap between molecular and aggregate states: how does molecular packing affect photophysical properties? *Chem. Eng. J.* **2023**, *451*, 138627.

17. Zhang, J.; Zhao, X.; Shen, H.; Lam, J. W. Y.; Zhang, H.; Tang, B. Z., White-light emission from organic aggregates: a review. *Adv. Photonics* **2021**, *4* (1), 014001.

18. Tang, S.; Yang, T.; Zhao, Z.; Zhu, T.; Zhang, Q.; Hou, W.; Yuan, W. Z., Nonconventional luminophores: characteristics, advancements and perspectives. *Chem. Soc. Rev.* **2021**, *50* (22), 12616-12655.

19. Wang, Y.; Nie, J.; Fang, W.; Yang, L.; Hu, Q.; Wang, Z.; Sun, J. Z.; Tang, B. Z., Sugar-Based Aggregation-Induced Emission Luminogens: Design, Structures, and Applications. *Chem. Rev.* **2020**, *120* (10), 4534-4577.

20. Li, M.; Li, X.; An, X.; Chen, Z.; Xiao, H., Clustering-Triggered Emission of Carboxymethylated Nanocellulose. *Front. Chem.* **2019**, *7*, 447.

21. Zhang, H.; Zhao, Z.; McGonigal, P. R.; Ye, R.; Liu, S.; Lam, J. W. Y.; Kwok, R. T. K.; Yuan, W. Z.; Xie, J.; Rogach, A. L.; Tang, B. Z., Clusterization-triggered emission: Uncommon luminescence from common materials. *Mater. Today* **2020**, *32*, 275-292.

22. Zhang, Z.; Yan, W.; Dang, D.; Zhang, H.; Sun, J. Z.; Tang, B. Z., The role of amide (n,π∗) transitions in polypeptide clusteroluminescence. *Cell. Rep. Phys. Sci.* **2022**, *3* (2), 100716.

23. Zhang, H.; Tang, B. Z., Through-Space Interactions in Clusteroluminescence. *JACS Au* **2021**, *1* (11), 1805-1814.

24. Zhang, H.; Zheng, X.; Xie, N.; He, Z.; Liu, J.; Leung, N. L. C.; Niu, Y.; Huang, X.; Wong, K. S.; Kwok, R. T. K.; Sung, H. H. Y.; Williams, I. D.; Qin, A.; Lam, J. W. Y.; Tang, B. Z., Why Do Simple Molecules with "Isolated" Phenyl Rings Emit Visible Light? *J. Am. Chem. Soc.* **2017**, *139* (45), 16264-16272.

25. Zhang, J.; Hu, L.; Zhang, K.; Liu, J.; Li, X.; Wang, H.; Wang, Z.; Sung, H. H. Y.; Williams, I. D.; Zeng, Z.; Lam, J. W. Y.; Zhang, H.; Tang, B. Z., How to Manipulate Through-Space Conjugation and Clusteroluminescence of Simple AIEgens with Isolated Phenyl Rings. *J. Am. Chem. Soc.* **2021**, *143* (25), 9565-9574.

26. Liu, J.; Zhang, H.; Hu, L.; Wang, J.; Lam, J. W. Y.; Blancafort, L.; Tang, B. Z., Through-Space Interaction of Tetraphenylethylene: What, Where, and How. *J. Am. Chem. Soc.* **2022**, *144* (17), 7901–7910.

27. Xiong, Z.; Zhang, J.; Wang, L.; Xie, Y.; Wang, Y.; Zhao, Z.; Zhang, H.; Zhi Sun, J.; Huang, F.; Tang, B. Z., Controllable Secondary Through-Space Interaction and Clusteroluminescence. *CCS Chemistry* **2023**, doi: 10.31635/ccschem.023.202302815.

28. Tu, W.; Xiong, Z.; Zhang, Z.; Zhang, J.; Wang, L.; Xie, Y.; Wang, Y.; Zhang, H.; Sun, J. Z.; Tang, B. Z., Manipulation of the through‐space interactions in diphenylmethane. *Smart Molecules* **2023**, *1*, e20220006.

29. Chu, B.; Zhang, H.; Chen, K.; Liu, B.; Yu, Q. L.; Zhang, C. J.; Sun, J.; Yang, Q.; Zhang, X. H.; Tang, B. Z., Aliphatic Polyesters with White-Light Clusteroluminescence. *J. Am. Chem. Soc.* **2022**, *144* (33), 15286-15294.

30. Chu, B.; Zhang, H.; Hu, L.; Liu, B.; Zhang, C.; Zhang, X.; Tang, B. Z., Altering Chain Flexibility of Aliphatic Polyesters for Yellow-Green Clusteroluminescence in 38 % Quantum Yield. *Angew. Chem. Int. Ed.* **2022**, *61* (6), e202114117.

31. Zhang, Z.; Xiong, Z.; Chu, B.; Zhang, Z.; Xie, Y.; Wang, L.; Sun, J. Z.; Zhang, H.; Zhang, X. H.; Tang, B. Z., Manipulation of clusteroluminescence in carbonyl‐based aliphatic polymers. *Aggregate* **2022**, *3*, e278.

32. Najbar, J.; Turek, A. M., Luminescence of naphthalene in an argon matrix. Geometry changes and multiplet structures. *Chem. Phys. Lett.* **1980**, *73* (3), 536-540.

33. Zhang, J.; Tu, Y.; Shen, H.; Lam, J. W. Y.; Sun, J.; Zhang, H.; Tang, B. Z., Regulating the proximity effect of heterocycle-containing AIEgens. *Nat. Commun.* **2023**, *14* (1), 3772.

34. Tu, Y.; Yu, Y.; Xiao, D.; Liu, J.; Zhao, Z.; Liu, Z.; Lam, J. W. Y.; Tang, B. Z., An Intelligent AIEgen with Nonmonotonic Multiresponses to Multistimuli. *Adv. Sci.* **2020**, *7* (20), 2001845.

35. Zhang, H.; Liu, J.; Du, L.; Ma, C.; Leung, N. L. C.; Niu, Y.; Qin, A.; Sun, J.; Peng, Q.; Sung, H. H. Y.; Williams, I. D.; Kwok, R. T. K.; Lam, J. W. Y.; Wong, K. S.; Phillips, D. L.; Tang, B. Z., Drawing a clear mechanistic picture for the aggregation-induced emission process. *Mater. Chem. Front.* **2019**, *3* (6), 1143-1150.

36. Shuai, Z.; Peng, Q., Organic light-emitting diodes: theoretical understanding of highly efficient materials and development of computational methodology. *Natl. Sci. Rev.* **2017**, *4* (2), 224-239.

37. Spackman, M. A.; Jayatilaka, D., Hirshfeld surface analysis. *CrystEngComm* **2009**, *11* (1), 19-32.

38. Spackman, P. R.; Turner, M. J.; McKinnon, J. J.; Wolff, S. K.; Grimwood, D. J.; Jayatilaka, D.; Spackman, M. A., CrystalExplorer: a program for Hirshfeld surface analysis, visualization and quantitative analysis of molecular crystals. *J. Appl. Crystallogr.* **2021**, *54*, 1006-1011.

39. Huang, H.; Yang, L.; Facchetti, A.; Marks, T. J., Organic and Polymeric Semiconductors Enhanced by Noncovalent Conformational Locks. *Chem. Rev.* **2017**, *117* (15), 10291-10318.

40. Huang, H.; Chen, Z.; Ponce Ortiz, R.; Newman, C.; Usta, H.; Lou, S.; Youn, J.; Noh, Y. Y.; Baeg, K. J.; Chen, L. X.; Facchetti, A.; Marks, T. J., Combining electron-neutral building blocks with intramolecular "conformational locks" affords stable, high-mobility p- and n-channel polymer semiconductors. *J. Am. Chem. Soc.* **2012**, *134* (26), 10966-73.

41. Zhang, J.; Zhang, H.; Lam, J. W. Y.; Tang, B. Z., Restriction of Intramolecular Motion(RIM): Investigating AIE Mechanism from Experimental and Theoretical Studies. *Chem. Res. Chinese Universities* **2021**, *37* (1), 1-15.